Journal of the Korean Nuclear Society
Volume 35, Number 6, pp.581~595, December, 2003

Monte Carlo Resonance Treatment for the Deterministic Transport Lattice Codes

Kang-Seog Kim, Chung Chan Lee, Moon Hee Chang, and Sung Quun Zee
Korea Atomic Energy Research Institute
150 Dukjin-dong, Yuseung-gu, Daejeon 305-353, Korea
kimks@kaeri.re.kr

(Received September 5, 2003)

Abstract

Transport lattice codes require the resonance integral tables for the resonant nuclides where the resonance integral is a function of the background cross section and can be prepared through a special program solving the slowing down equation. In case the cross section libraries do not include the resonance integral table for the resonant nuclides, the computational prediction produces a large error. We devised a new method using a Monte Carlo calculation for the effective resonance cross sections to solve this problem provisionally. We extended this method to obtain the resonance integral table for general purpose. The MCNP code is used for the effective resonance integrals and the LIBERTE code for the effective background cross sections. We modified the HELIOS library with the effective cross sections and the resonance integral tables obtained by the newly developed Monte Carlo method, and performed sample calculations using HELIOS and LIBERTE. The results showed that this method is very effective for the resonance treatment.

Key Words : resonance integral table, transport lattice codes, monte-carlo, MCNP, HELIOS, LIBERTE

1. Introduction

It is very inefficient and time-consuming to use point-wise cross sections in a deterministic transport calculation. Therefore, typically 30 to 70 energy discretized cross sections are used in the calculation, which are processed from the ENDF/B-VI library using the NJOY program [1]. The multi-group cross section is calculated by flux weighting. The accuracy of a deterministic transport calculation is mainly dependent upon the scalar flux and group width. Therefore, energy groups and spectra should be chosen such that the library cross sections are insensitive to the variations of the flux spectra in their anticipated range of application. The existence of resonance makes this treatment very complicated, in which the incident energy of a neutron matches one of the excited energy levels of the compound nucleus. The energy discretized cross sections at

the energy range except the resonance are insensitive to the scalar flux and energy groups.

The resonance behavior of the absorption cross section complicates the evaluation of group cross sections. The scalar flux will have dips at and near the resonance energies due to the resonance. These dips depend on the resonances and the concentration of the resonance isotopes and on their location. The cross sections of other nuclides without resonances can be affected because of the flux weighted averaging.

There are three possible methods for the resonance treatment to obtain effective resonance integrals. These are the Bondarenko method [2], flux calculation method and the calculation of the detailed spectra in the resonance region by a special program. The first two methods are included in the NJOY program. The third one is the standard procedure to reduce the errors in predicting the effective resonance cross sections. Therefore we focus on the third method in this paper.

The effective resonance cross sections can be affected by the self shielding effect by resonance itself, resonance interference with the other resonant nuclides, and geometrical configurations. In general, the resonance integrals are tabularized as a function of the background cross section to be applied to any combination of affecting factors. The resonance integral table is prepared through the calculation of the slowing down equation for the heterogeneous cylindrical fuel pins using a special program such as RABBLE [3].

Occasionally when the resonant nuclides are not treated as a resonant nuclide, the resonance integral tables for these nuclides are excluded from the neutron cross section library for the transport lattice code. This may cause a relatively large error in the transport lattice calculations. In order to solve this problem provisionally the effective resonance cross sections for the specified geometry and composition should be used instead. Another way is to include the resonance integral table and to treat this nuclide as a resonant one.

The objective of our research is to develop a simple and effective method to obtain the effective resonance cross sections provisionally or generally. In this research we developed new provisional and general methods to prepare the effective resonance cross section using a Monte Carlo calculation.

The provisional method is to obtain the effective resonance cross section for the specified composition and geometrical configurations directly from a Monte Carlo calculation. The general method is to prepare the resonance integral tables using Monte Carlo calculations for the effective resonance cross sections and heterogeneous transport calculations for the background cross sections. We used MCNP [4] as a Monte Carlo code and LIBERTE [5] developed at KAERI as a transport lattice code.

2. Methodology

2.1. Conventional Resonance Treatment

The resonance integrals are tabularized as a function of various background cross sections and temperatures for the extended applications. The background cross section is expressed as follows:

$$\sigma_b = \lambda\sigma_p + \sigma_e, \quad (1)$$

where λ is the hydrogen-equivalence factor also called the intermediate resonance factor, σ_p the potential scattering cross section and σ_e the equivalence cross section. The hydrogen-equivalence factor for hydrogen has been defined as 1.0, and those for the other isotopes have been obtained by comparing the solutions in U^{238}/H mixtures with mixtures where the hydrogen was partly replaced by the other isotopes.[6] Since λ

depends on the resonance width, the library includes group dependent λ values.

The slowing-down equation [7] at resonance lethargies, and away from fission sources, is

$$\Sigma(u)\,\phi(u) = Q(u), \tag{2}$$

and

$$Q(u) = \int_{u-\Delta}^{u} \Sigma_s(u')\phi(u')\frac{\exp(u'-u)}{1-\alpha}du'. \tag{3}$$

where

$$\left.\begin{aligned} \Sigma_s(u) &= \Sigma_p + \Sigma_{rs}(u) \\ \Sigma(u) &= \Sigma_s(u) + \Sigma_a(u) \\ \alpha(u) &= (A-1)^2/(A+1)^2 \\ \Delta &= -\ln(\alpha) \end{aligned}\right\}, \tag{4}$$

the source $Q(u)$ is exclusively due to slowing-down, $\Sigma_s(u)$ is the macroscopic scattering cross section, $\Sigma(u)$ is the macroscopic total cross section; 1-α is the maximum fractional energy loss per collision with an isotope of mass A, and Δ is the maximum lethargy gain per collision with an isotope of mass A.

The intermediate resonance (IR) approximation [8] assumes that the lethargy gain per collision is greater than the practical resonance width (the narrow resonance) at the fraction λ of its scattering.[6] Using $\Sigma_s(u)=\lambda\Sigma_p$ and $\phi(u)=1$ outside the resonance, the source $Q(u)$ in eq. (3) can be

$$Q(u) = \lambda\Sigma_p \int_{u-\Delta}^{u} \frac{\exp(u'-u)}{1-\alpha}du'. \tag{5}$$

If the integration interval (Δ) is very small, the integration can be approximated to 1.0 and the source $Q(u)$ will be $\lambda\Sigma_p$. The remaining fraction, $(1-\lambda)\Sigma_p$, does not provide a source neutron from outside the resonance width because the resonance is so wide that the neutron can not gain enough lethargy. This is considered to be due to self-scattering which neither adds nor removes neutrons. We have the solution for eq. (2) using the simplified source as follows:

$$\phi(u) = \frac{\lambda\Sigma_p}{\Sigma_a(u) + \lambda\Sigma_p}. \tag{6}$$

Since the scalar fluxes obtained in eq. (6) do not consider the geometrical configuration, these can not be directly applicable. Considering the geometrical leakage, we can use the heterogeneous transport equation at the resonance energy range as follows:

$$\begin{aligned} &\hat{\Omega}\cdot\nabla\varphi(\vec{r},\hat{\Omega},u) + (\Sigma_a(\vec{r},u) + \lambda(u)\Sigma_p(\vec{r}))\varphi(\vec{r},\hat{\Omega},u) \\ &\quad = \lambda(u)\Sigma_p(\vec{r}). \end{aligned} \tag{7}$$

Eq. (7) is used in calculating the equivalence cross section with the associated geometrical configuration. The equivalence theory between the infinite homogeneous and heterogeneous problems is as follows:

$$\Sigma_b = \lambda\Sigma_p \quad \Leftrightarrow \quad \Sigma_b = \lambda\Sigma_p + \Sigma_e. \tag{8}$$

The equivalence cross section is mainly dependent upon the geometrical configuration of the fuel pins. The correspondent transport equation to eq. (8) is

$$\begin{aligned} &(\Sigma_a(\vec{r},u) + \lambda(u)\Sigma_p(\vec{r}) + \Sigma_e(\vec{r}))\varphi(\vec{r},\hat{\Omega},u) \\ &\quad = \lambda(u)\Sigma_p(\vec{r}) + \Sigma_e(\vec{r}). \end{aligned} \tag{9}$$

Using eq. (8), the solution is

$$\phi(\vec{r},u) = \frac{\Sigma_b(\vec{r},u)}{\Sigma_a(\vec{r},u) + \Sigma_b(\vec{r},u)}. \tag{10}$$

Since the resonance cross sections are tabularized as functions of microscopic background cross section and temperature, we have to change the background cross section into a micro form. When N_i is the number density of the only resonance isotope in the mixture, the microscopic background cross section of this mixture is

$$\sigma_{b,r} = \frac{1}{N_r}\left(\sum_{i=1}^{N} N_i \lambda_i \sigma_{pi} + \Sigma_e\right) = \frac{1}{N_r}(\lambda\Sigma_p + \Sigma_e) \,. \quad (11)$$

Using the above background cross section, the resonance cross sections are read from the library. The first term in eq. (11) can be obtained directly from smooth data in the library. The equivalence cross section can be obtained through the fuel-to fuel collision probability. [9, 10] We introduce the procedure to calculate the effective and the equivalence cross sections in the RABBLE code.

The RABBLE code is used to compute the resonance absorption in cylindrical fuel cells. The cell is divided into flat flux regions, and the energy range of interest is divided into extremely narrow lethargy intervals. Regional fluxes and reaction rates are obtained from the slowing down sources and the first flight collision probabilities (or transmission and escape probabilities). These regional reaction rates are accumulated over specified multi-group structures to yield effective cross sections. The equivalence cross section can be obtained by the following equations.

$$\Sigma_e = N_i \alpha \sigma_{xi}, \quad (12)$$

where

$$\left.\begin{aligned} b &= \frac{\gamma}{N_i \ell}\Big/\left(5.0 + \frac{\lambda\Sigma_p}{N_i}\right) \\ a &= \frac{1.0 + 2.71 \cdot b}{1.0 + 2.34 \cdot b} \\ \sigma_{xi} &= \frac{a}{N_i \ell} \\ \alpha &= \frac{\beta - (1-\gamma)}{\beta - (1-a)(1-\gamma)}, \beta = 1.0 \end{aligned}\right\}, \quad (13)$$

N_i is the number density of the resonance material i, a the Bell factor, l the mean chord length (two times the fuel radius) and γ the Dancoff factor [11].

For each resonance isotope and in each resonance group, the library contains tables of absorption (and ν·fission if fissionable) cross sections from resonance integrals as functions of temperature and background cross sections. The absorption and ν·fission resonance integrals are linear in $\sqrt{T}$, where the temperature dependency is due to the Doppler effect. While the temperature dependency is simple, the background cross section dependency is very complicated. So the method of Segev [12] is used to interpolate the resonance integral divided by the group width Δu (R values). For simplicity we call the R value the resonance integral in this paper.

The resonance cross sections can be related with the resonance integrals using the following equations:

$$\sigma_a = \frac{R(\sigma_b)}{1 - R(\sigma_b)/\sigma_b}, \quad (14)$$

$$\nu\sigma_f = \frac{R_\nu(\sigma_b)}{1 - R_\nu(\sigma_b)/\sigma_b}. \quad (15)$$

2.2. The Subgroup Method [16]

The subgroup method was developed by Khairallah and Recolin [13], Roth [14], and Notari and Garraffo [15]. The essential factor is that the resonance integral divided by the group width is approximated by quadratures. Since the background cross section is constant within a group, eq. (10) can be written with microscopic ones as follows:

$$\phi(u) = \frac{\sigma_b}{\sigma_a(u) + \sigma_b}. \quad (16)$$

The lethargy dependency of the flux of eq. (16) is uniquely through $\sigma_a(u)$. It allows to replace the integration variable u by σ_a and to approximate the integrals by quadratures in σ_a according to the following equations:

$$\frac{1}{\Delta u}\int_{\Delta u} f(u)du = \frac{1}{\Delta u}\int_{\Delta u} f(\sigma_a)\frac{du}{d\sigma_a}d\sigma_a \cong \sum_n w_n f_n, \quad (17)$$

where $f_n=f(\sigma_n)$ are the integrands at the discrete values of σ_a. The resonance cross section is subdivided with σ_{an}' s over the σ_a range and their weights (w_n). The condition for the weights is

$$\sum_n w_n = 1 \quad and \quad 0 \le w_n \le 1. \tag{18}$$

Therefore the effective resonance cross section can be approximated by the quadrature set of σ_{an} and w_n as follows:

$$\sigma_a = \frac{\sum_n w_n \sigma_{an} \phi_n}{\sum_n w_n \phi_n}. \tag{19}$$

The absorption cross sections σ_{an} are arbitrarily chosen and the number of the subgroup is determined as having the accurate effective cross sections. If a good set of σ_{an} values is known, the corresponding weights (w_n) are obtained from the heterogeneous resonance integral tables using a least-square fitting. Using eqs. (16) and (19), we can obtain the following relationship:

$$\sigma_a = \frac{\sum_{n=1}^{N} w_n \sigma_{an} \frac{\sigma_b}{\sigma_{an}+\sigma_b}}{\sum_{n=1}^{N} w_n \frac{\sigma_b}{\sigma_{an}+\sigma_b}}. \tag{20}$$

Eq. (20) can be rewritten with the resonance integral as follows:

$$R(\sigma_b) = \frac{RI(\sigma_b)}{\Delta u} = \sigma_a \sum_n w_n \frac{\sigma_b}{\sigma_{an}+\sigma_b} = \sum_n w_n \sigma_{an} \frac{\sigma_b}{\sigma_{an}+\sigma_b}. \tag{21}$$

If the medium is infinitely dilute, the flux in eq. (21) is constant. So we obtain the following equation:

$$R(\sigma_\infty) = \sum_n w_n \sigma_{an}. \tag{22}$$

σ_{an} values are chosen to be independent upon the temperature, but the weights are varied with the temperature. The weights for a specified temperature are obtained by the simple linear interpolation according to $\sqrt{T}$.

Eq. (19) is used to calculate the effective resonance cross section. The corresponding scalar flux ϕ_n is unknown and has to be obtained from the heterogeneous transport calculations. However, we use eq. (20) as a detour via σ_b instead of directly using the fluxes ϕ_n because of the weak dependency of σ_b on σ_a and the necessity of dealing with interacting resonance isotopes.

The heterogeneous transport calculations are used to obtain the background cross sections by the following relationship:

$$\phi_n = \frac{\sigma_{bn}}{\sigma_{an}+\sigma_{bn}} \Rightarrow \sigma_{bn} = \frac{\sigma_{an}\phi_n}{1-\phi_n}. \tag{23}$$

If we know the corresponding background cross section σ_{bn} to σ_{an} , the effective resonance cross section can be obtained by eq. (24).

$$\sigma_a = \frac{\sum_{n=1}^{N} w_n \sigma_{an} \frac{\sigma_{bn}}{\sigma_{an}+\sigma_{bn}}}{1-\sum_{n=1}^{N} w_n \frac{\sigma_{an}}{\sigma_{an}+\sigma_{bn}}}. \tag{24}$$

The $\nu\cdot$fission cross section is also evaluated from eq. (25).

$$\nu\sigma_f = \frac{\sum_n w_{\nu n} \sigma_{\nu fn} \frac{\sigma_{bn}}{\sigma_{an}+\sigma_{bn}}}{1-\sum_n w_n \frac{\sigma_{an}}{\sigma_{an}+\sigma_{bn}}}. \tag{25}$$

The heterogeneous transport calculations are performed with the corresponding absorption cross section (σ_{an}) as follows:

$$\hat{\Omega}_m \cdot \nabla \varphi_m(\vec{r}) + \Sigma_{rn}(\vec{r}) \varphi_m(\vec{r}) = Q(\vec{r}), \tag{26}$$

where

$$\left.\begin{aligned} Q &= \sum_i \lambda_i N_i \sigma_{pi} \equiv \lambda \Sigma_p \\ \Sigma_{rn} &= N\sigma_{an} + \lambda\Sigma_p = \Sigma_{an} + \lambda\Sigma_p \end{aligned}\right\}, \tag{27}$$

m denotes the angle and n the number of the subgroup. Eq. (26) is solved by the same method used in the main transport calculation. If we know the scalar flux, we calculate the corresponding background cross sections to σ_{an} using the following equation:

$$\Sigma_b(\sigma_{an}) = \frac{\Sigma_a(\sigma_{an})\phi_n}{1-\phi_n}. \quad (28)$$

2.3. Provisional Resonance Treatment

Cross section library for the transport lattice code includes the resonance integral tables for the resonant nuclides. However, resonance integral tables are not provided for some nuclides, which causes problems for the accurate predictions of reactor physics parameters. Since the structures for most of the cross section libraries are complicated and the cross section data is closely related with each other, it is very time consuming to include the additional data such as the resonance integral table. It is required that the cross sections for the resonant nuclide should be thus easily replaced with the appropriate effective ones. These effective resonance cross sections should include the effects from the self-shielding effect by the resonance itself, resonance interferences with other resonant nuclides and the geometrical configuration.

We suggest that the effective resonance cross sections can be evaluated through the Monte Carlo calculations. Since Monte Carlo codes such as the MCNP for the neutron transport calculation use the continuous cross section over energy, there is no approximation for the resonance calculation. The effective microscopic resonance cross sections can be obtained through the flux and microscopic reaction rate tallies for the regions with resonant nuclides.

$$\sigma_{xg} = \frac{\int_{\Delta E_g} \sigma_x(E)\phi(E)dE}{\int_{\Delta E_g} \phi(E)dE} \quad (29)$$

Monte Carlo calculations for the multiplication factor are performed with the specified geometry and composition assuming the infinite arrays of a fuel pin, assembly or other repeated geometry.

Since the effective resonance cross section is dependent upon the geometrical configuration and composition of the surrounding materials, the basic geometry for the array should be chosen carefully to minimize the errors originated from the difference between the conditions for the cross section generation and for the application. For instance, if the resonant nuclide is commonly included in the fuel pins, the infinite array of fuel pin can be chosen. If the resonant nuclide is in the control rod, the MCNP calculation should be performed for the fuel assembly.

2.4. General Resonance Treatment

The general resonance treatment is an extension of the provisional treatment mentioned in the previous section, to include the resonance integral table prepared by the Monte Carlo calculations. This procedure includes two parts that are a Monte Carlo calculation with various geometries and compositions, and the generation of the corresponding background cross section.

MCNP for the Monte Carlo calculations can be used to obtain the effective resonance cross sections for the specified resonance energy groups instead of using RABBLE. In the conventional procedure of the RABBLE calculation, it is assumed that the fuel is composed of U^{235}, U^{238} and O^{16}, and the cladding is natural zirconium, and the moderator is water. When calculating the resonance calculation of U^{235} or U^{238}, the other nuclides include only potential scattering cross

sections as background material to exclude the resonance interference effects. The effective background cross section can be obtained from the summation of the potential cross sections multiplied by the hydrogen equivalent factor and the equivalence cross section from the Dancoff factor. So as to change the background cross sections three components are varied, which include the void fraction, fuel rod pitch and the amount of uranium in the fuel.

In order to remove the resonance interference between the resonance nuclides, MCNP cross section libraries of U^{235} and U^{238} with only scattering cross sections should be prepared, which are used for the background nuclides.

In the conventional resonance treatment of Section 2.1, the equivalence cross section is calculated from the Dancoff factor. If the Dancoff factor is also used to obtain the effective resonance integral in the transport lattice calculation, there will be a consistency between the generation of a resonance integral table and the retrieval of the resonance integral in a lattice calculation. Although the Dancoff factor is used for the equivalence cross section in the lattice code, this factor is not generated explicitly. One of the merits of the subgroup method is to overcome this kind of problem. However, the subgroup data of HELIOS is generated from the conventional method of the resonance treatment. Since there is an inconsistency between the preparation and the use of the library, we suggest a new method for consistency. In this research the background cross sections are obtained through the resonance transport calculation for a single pin using eq. (26). We used the LIBERTE code [5] developed at KAERI which adopts the characteristics method for the spatial discretization and the subgroup method for the resonance treatment.

The flow diagram for the preparation of a cross section library is shown in Figure 1. As shown in the figure, the procedure begins with processing the ENDF/B-VI library using the NJOY code package [1]. The conventional procedure includes NJOY processing for the discretized multi-group cross sections for the resonant nuclides. However, this procedure includes NJOY processing for the continuous MCNP cross sections for the resonance nuclides. MCNP calculations are performed by changing the void fraction, fuel to moderator volume ratio and the amount of fuel material. The effective cross sections are obtained for the non-resonance energy groups, and the various resonance integrals for the resonance

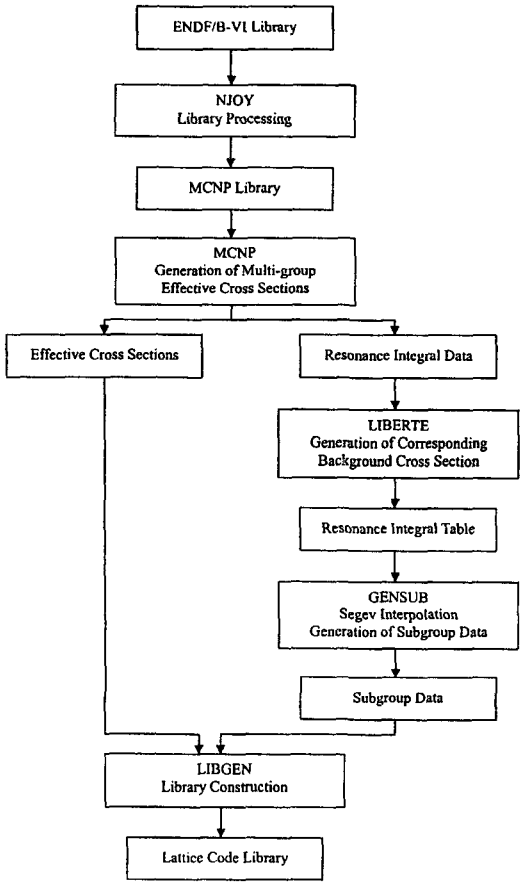

Fig. 1. Flow Chart for the Generation of Cross Section Library

energy groups. Then, the effective background cross sections are obtained through the resonance transport calculations to complete the resonance integral table. Using these resonance integral tables, the number of data sets can be increased by the Segev interpolation. The subgroup data can be obtained from the resonance integral table using the GENSUB program. The effective cross sections, the resonance integral tables and the subgroup data for each nuclide are combined together to construct the cross section library using the LIBGEN program.

3. Calculation

3.1. Provisional Resonance Treatment

We selected two sets of sample problems to see the effectiveness of the provisional resonance treatment method using a Monte Carlo calculation. One of the sample problems includes highly enriched (80% U^{235}) fuel rods in the form of uranium dioxide with copper.[7] The other one is to include intermediately enriched (20% U^{235}) fuel rods of uranium-zirconium alloy which are arbitrarily constructed including the same geometry as the first one. The detailed descriptions for these fuel rods are shown in Table 1.

As shown in Figures 2 and 3, copper and zirconium include strong resonances at the energy between 10^2~10^5 eV. Since these resonances are not treated explicitly in the HELIOS-1.7 library, the effective resonance cross sections should be evaluated through MCNP calculations. We compared the multiplication factors of HELIOS using the old and the new library by replacing the effective cross sections in the resonance energy groups. We adopt 45 energy groups used in HELIOS-1.7 as shown in Table 2. The resonance energy groups are 16 groups from group-10 to group-25 of which the energy range is 1.8554 ~ 9118.8 eV.

Table 1. Fuel Rod Specifications

Item	Set-1	Set-2
Fuel rod pitch (cm)	0.530	0.530
Rod geometry	hexagonal	hexagonal
Cladding outer radius (cm)	0.1965	0.1965
Fuel outer radius (cm)	0.1651	0.1651
Fuel		
- density (g/cm^3)	8.112	7.860
- U^{235} enrichment (w/o)	80	20
- material	UO_2+Cu	U+Zr
- temperature (K)	300	300
Cladding		
- density (g/cm^3)	7.0	7.0
- material	SS	SS
- temperature (K)	300	300
Moderator		
- density (g/cm^3)	0.9981	0.9981
- material	H_2O	H_2O
- temperature (K)	300	300

Table 2. Group-wise Energy Boundaries

gr	Upper	Lower	gr	Upper	Lower	gr	Upper	Lower
1	2.0000E+1	6.0653E+0	16	1.3710E-5	1.2099E-5	31	1.0137E-6	9.7100E-7
2	6.0653E+0	3.6788E+0	17	1.2099E-5	8.3153E-6	32	9.7100E-7	9.1000E-7
3	3.6788E+0	2.2313E+0	18	8.3153E-6	7.3382E-6	33	9.1000E-7	7.8208E-7
4	2.2313E+0	1.3534E+0	19	7.3382E-6	6.4760E-6	34	7.8208E-7	6.2506E-7
5	1.3534E+0	8.2085E-1	20	6.4760E-6	5.7150E-6	35	6.2506E-7	3.5767E-7
6	8.2085E-1	4.9787E-1	21	5.7150E-6	5.0435E-6	36	3.5767E-7	2.7052E-7
7	4.9787E-1	1.8316E-1	22	5.0435E-6	4.4509E-6	37	2.7052E-7	1.8443E-7
8	1.8316E-1	6.7379E-2	23	4.4509E-6	3.9279E-6	38	1.8443E-7	1.4572E-7
9	6.7379E-2	9.1188E-3	24	3.9279E-6	2.3824E-6	39	1.4572E-7	1.1157E-7
10	9.1188E-3	2.0347E-3	25	2.3824E-6	1.8554E-6	40	1.1157E-7	8.1968E-8
11	2.0347E-3	1.3007E-4	26	1.8554E-6	1.4574E-6	41	8.1968E-8	5.6922E-8
12	1.3007E-4	7.8893E-5	27	1.4574E-6	1.2351E-6	42	5.6922E-8	4.2755E-8
13	7.8893E-5	4.7851E-5	28	1.2351E-6	1.1254E-6	43	4.2755E-8	3.0613E-8
14	4.7851E-5	2.9023E-5	29	1.1254E-6	1.0722E-6	44	3.0613E-8	1.2396E-8
15	2.9023E-5	1.3710E-5	30	1.0722E-6	1.0137E-6	45	1.2396E-8	0.0000E+0

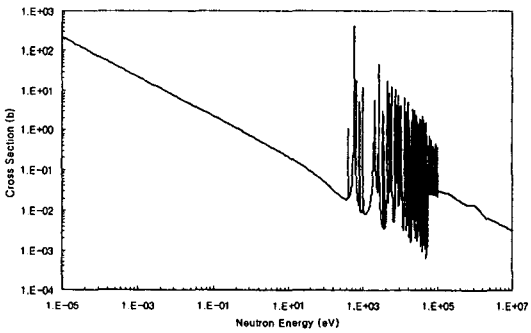

Fig. 2. Radiative Capture Cross Section for Cu^{63}

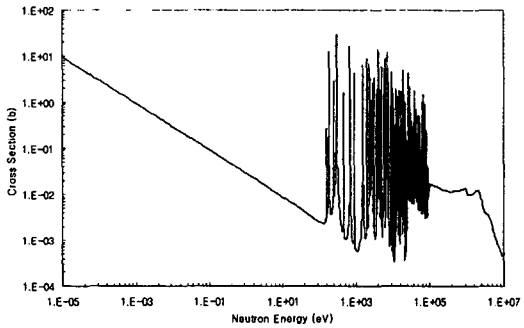

Fig. 3. Radiative Capture Cross Section for Zr^{nat}

3.2. General Resonance Treatment

Resonance integral tables are generated through the MCNP calculations for the typical fuel pin of the pressurized water reactor. The geometrical dimension and composition for the fuel pin are listed in Table 3. In order to change the background cross section, three factors shown in Table 4 are introduced, which include the volume of the moderator, void fraction and the particle number density of the fissile nuclides. The factor 'n' is a dividing factor for the original particle number densities of U^{235} and U^{238}. Temperatures for the cladding and the moderator are fixed at the

Table 3. Fuel Rod Specifications

Item	Dimension
Fuel rod pitch (cm)	1.33171 (variable, refer to Table 4)
Rod geometry	Rectangular
Cladding outer radius (cm)	0.4759
Fuel outer radius (cm)	0.4025
Fuel pellet	
- density (g/cm^3)	10.4 (variable, refer to Table 4)
- U^{235} enrichment (w/o)	5.0
- Material	UO_2
- Temperature (K)	300
Cladding	
- density (g/cm^3)	6.55
- material	$Zr^{nat.}$
- Temperature (K)	600
Moderator	
- density (g/cm^3)	0.6591 (variable, refer to Table 4)
- material	H_2O
- Temperature (K)	600

Table 4. Factors to Change the Background Cross Sections

Case	1	2	3	4	5	6	7	8	9
Vm/Vf	1.0	1.0	1.0	1.0	2.0	4.0	4.0	4.0	4.0
Void Fraction (%)	90.0	80.0	40.0	0.0	0.0	0.0	0.0	0.0	0.0
n	1.0	1.0	1.0	1.0	1.0	1.0	2.0	4.0	8.0

condition of a hot full power and only the fuel temperature is varied such that the cross section library for the lattice code can be the best at the operating full power condition. For this purpose we set the temperatures of the cladding and moderator to 600 K and the fuel temperature to 300 K.

MCNP calculations are performed to obtain the effective resonance cross sections of U^{235} and U^{238} by changing three factors. Scalar fluxes, microscopic absorption and the fission reaction rates, and the number of neutrons released from fission are tallied for the fuel region. Since the interference between the resonant nuclides is to be considered in the subgroup calculation, this effect must be excluded from the generation of a resonance integral table. U^{235} and O^{16} are background nuclides for the U^{238}calculation and U^{238} and O^{16} are the background nuclides for U^{235}calculation, where the MCNP libraries with only scattering cross sections are used for the background nuclides.

The corresponding background cross sections are calculated using the obtained effective resonance cross sections through the resonance transport calculation by use of the LIBERTE code. The obtained resonance cross section tables with 9 data points can be extended to the tables with

16 data points using the Segev interpolation. These resonance integral tables are transformed into the subgroup data.

4. Result and Discussion

4.1. Provisional Resonance Treatment

We compared the effective resonance absorption cross sections of Cu^{63}, Cu^{65} and $Zr^{nat.}$ from MCNP calculations with those from the HELIOS library. Absorption cross sections match well with each other except groups 9, 10 and 11. Effective absorption cross sections of groups 9, 10 and 11 are compared with each other in Table 5. The effective cross sections are reduced significantly at these resonance energy groups. Decrease in the effective absorption cross section is due to the resonance self-shielding and the interference with the resonant nuclides of U^{235} and U^{238}.

We compared the multiplication factors of the HELIOS calculations with the old and new library with those of MCNP to see the effectiveness of this method in Table 6. When using the old HELIOS library, the reactivity differences between HELIOS and MCNP are about 5000 pcm for copper and 500 pcm for zirconium. However,

Table 5. Comparison of the Effective Absorption Cross Sections

Nuclide	Group	Old	New	Diff.(%)
Cu63	9	8.545861E-02	6.900105E-02	19.3
	10	3.779660E-01	1.786221E-01	52.7
	11	8.489397E-01	2.335263E-01	72.5
Cu65	9	3.881821E-02	3.424761E-02	11.8
	10	2.069747E-01	1.294865E-01	37.4
	11	3.089572E-01	1.960521E-01	36.5
Zrnat.	9	3.230754E-02	2.893119E-02	10.5
	10	1.317450E-01	9.610002E-02	27.1
	11	2.028490E-01	1.305671E-01	35.6

Table 6. Comparison of the Multiplication Factors for Single Pin Calculation

Code & Library	Set-1		Set-2	
	Keff	Diff. (pcm)	Keff	Diff. (pcm)
MCNP	1.54421 ±0.00034	-	1.48508 ±0.00034	-
HELIOS Old *	1.49568	4853	1.48006	502
HELIOS Old †	1.49377	5044	1.47938	570
HELIOS New *	1.54550	-129	1.48580	-72
HELIOS New †	1.54396	25	1.48513	-5

* : Option for resonance calculation of (111111111)

† : Option for resonance calculation of (444444444)

using the new library, the reactivity differences are reduced to about 100 pcm for both cases with the resonance option of a fine-group resonance transport calculation using a representative nuclide of U^{235}. When we selected U^{238} as a representative nuclide, the reactivity difference is less than 25 pcm.

We can perform these calculations by changing the temperatures and generate the provisional resonance table as a function of temperature. Although the effective cross sections should be restricted to the specified geometrical structure and composition, this method is quite simple and effective as a provisional substitute.

4.2. General Resonance Treatment

At first we reviewed the variation of the effective cross sections for the non-resonance energy groups. Figure 4 shows the group-wise RMS error distributions for the absorption and $\nu\cdot$fission cross sections of U^{235} and absorption cross sections of U^{238}. As shown in the figure, RMS errors are small for the non-resonance groups except group-35 of U^{235}. The reason is that U^{235} includes the resonance for this energy group. However, this resonance can not be treated explicitly because this is a non-resonance energy group. We selected the effective cross sections of case 4 as a representative to be used in the sample calculation.

We obtained the resonance integral table through the MCNP and LIBERTE calculations. In order to compare the new resonance integrals with those of the HELIOS library, we performed Segev interpolations for 16 background cross sections given in the HELIOS library. Figures 5 and 6 show the comparison of the absorption and $\nu\cdot$fission resonance integrals from HELIOS and our method at σ_b=831 b. There are slight differences at the resonance peaks between HELIOS and new libraries. Figure 7 shows the comparison of the absorption resonance integrals from HELIOS and our method at σ_b=739 b. There is also a slight difference at the resonance peak between HELIOS and the new libraries.

We compared the absorption and $\nu\cdot$fission resonance integrals of U^{235} as a function of the background cross section for group-7 in Figures 8 and 9. We also compared the absorption resonance integrals of U^{238} as a function of the background cross section for group-10 in Figure 10. The curves are slightly different from each other. The fact that the infinite resonance integrals are different from

Table 7. Comparison of the Multiplication Factors

Case	MCNP	LIBERTE			
		Old Lib.	Diff.(pcm)	New Lib.	Diff.(pcm)
1	0.94471 (0.00039)	0.95767	-1296	0.94330	141
2	1.06889 (0.00023)	1.08030	-1141	1.06494	395
3	1.33757 (0.00025)	1.34336	-579	1.33325	432
4	1.44586 (0.00022)	1.44974	-388	1.44257	329
5	1.50130 (0.00020)	1.50386	-256	1.49819	311
6	1.52412 (0.00020)	1.52727	-315	1.52210	202
7	1.44787 (0.00017)	1.45249	-462	1.45137	-350
8	1.01608 (0.00012)	1.02124	-516	1.01477	131

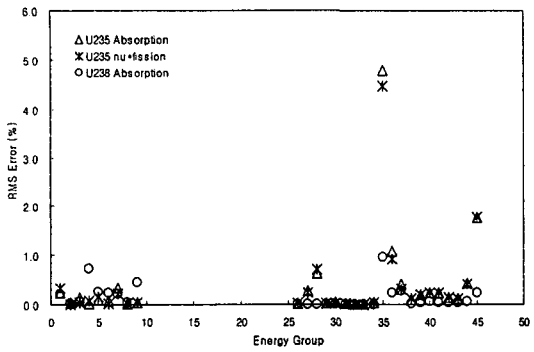

Fig. 4. Distribution of RMS Errors for Non-resonance Energy Groups

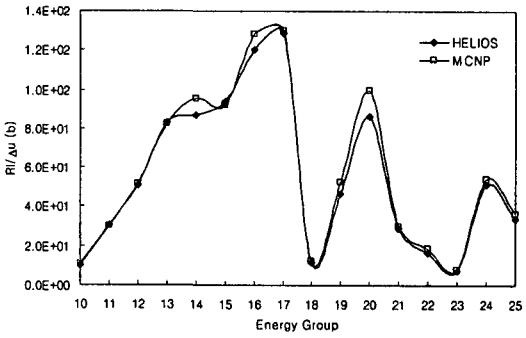

Fig. 6. Comparison of ν·fission Resonance Integral of U^{235} (σ_b=831 b)

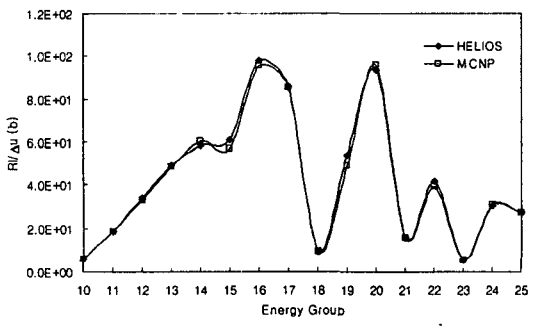

Fig. 5. Comparison of Absorption Resonance Integral of U^{235} (σ_b=831 b)

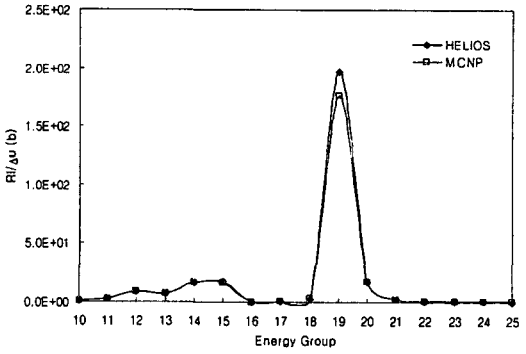

Fig. 7. Comparison of Absorption Resonance Integral of U^{238} (σ_b=739 b)

each other is due to the use of different ENDF/B libraries for the HELIOS and MCNP.

The subgroup data was generated through the Segev interpolation and the least square fitting to minimize RMS errors. In the present study we used the same subgroup σ_{an} with HELIOS and found the weightings. We modified the resonance integral tables, subgroup data and the effective absorption and ν·fission cross sections for U^{235} and U^{238} as given in section 2.

We performed the same sample calculations with the cases for the generation of the resonance integral tables by MCNP and LIBERTE. We compared the multiplication factors of the LIBERTE calculations with HELIOS and the new libraries with those of MCNP. As shown in Table 7, LIBERTE with the new library predicts the multiplication factors better for most cases. However, LIBERTE with new library overestimated the multiplication factor only for case 7, but it is still closer to the MCNP value. Especially for the cases with low background cross sections, there is a significant improvement in predicting the multiplication factors. It is noted that this improvement mainly comes from the consistency in the generation of the background cross sections between the preparation of the resonance integral table and the real application.

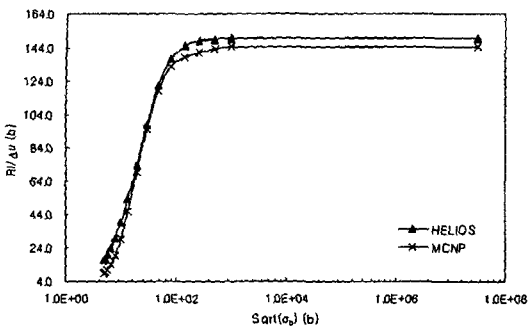

Fig. 8. Absorption Resonance Integral of U^{235} as a Function of σ_b (group-7)

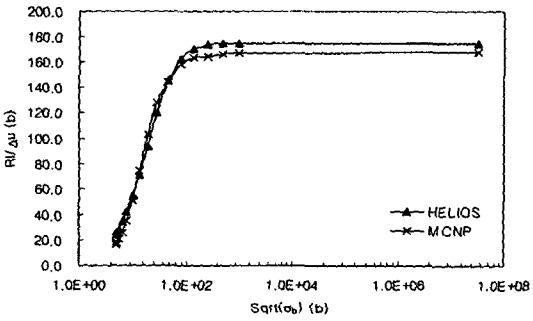

Fig. 9. ν -fission Resonance Integral of U^{235} as a Function of σ_b (group-7)

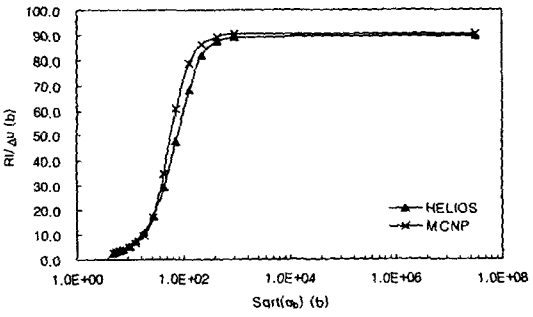

Fig. 10. Absorption Resonance Integral of U^{238} as a Function of σ_b (group-10)

The results showed that the new resonance treatment method using a Monte Carlo calculation can be a good substitute for the conventional method.

5. Conclusions

We proposed a new resonance treatment method which includes provisional and general treatments using Monte Carlo calculations. When the resonant nuclides are treated improperly in the library for the lattice codes, the library can be easily modified using the new provisional resonance treatment method to obtain a reasonable solution. It is very convenient to cope with the trouble of resonant nuclides in the cross section libraries for the transport lattice codes in many real applications.

The resonance integral tables could be obtained properly using the MCNP and the transport lattice codes such as LIBERTE. The background cross sections by our new method maintain the consistency between the procedure of the preparation of the resonance integral table and that of the retrieval of the effective resonance integral. The results showed that the new resonance treatment method for the transport lattice calculations works well compared to the conventional method.

References

1. "NJOY91.118 : A Code System for Producing Pointwise and Multigroup Neutron and Photon Cross Sections from ENDF/B Evaluated Nuclear Data," ORNL, RSIC, PSR-171 (1994).
2. I. I. Bondarenko and et al., "Group Constants for Nuclear Reactor Calculations," Consultant Bureau, New York (1964).
3. P. H. Kier and et al., "RABBLE, A Program for Computation of Resonance Absorption in Multiregion Reactor Cells, " ANL-7326 (1967).
4. J. F. Breismeister and et al., "MCNP - A General Monte Carlo N-Particle Transport Code, Version 4B," LA-12625-M (1997).
5. K. S. Kim and et al., "Development of DENT

2D Code Based on the Characteristics Method," *Trans. Am. Nuc. Soc.* , 86, 369-371 (2002).

6. A. C. Aldous, "Numerical studies of the hydrogen equivalent of some structural materials in their effect on U-238 resonance capture," *UKAEA Report AEEW-M* 860, Winfrith, England (1969).
7. A. M. Weinberg and E. P. Wigner, "The Physical Theory of Neutron Chain Reactors," The University of Chicago Press (1958).
8. R. Goldstein and E. R. Cohen, "Theory of resonance absorption of neutrons," *Nucl. Sci. Eng.* 13, 132-140 (1962).
9. M. Edenius and et al., "CASMO-3, A Fuel Assembly Burnup Program Methodology Version 4.4," STUDSVIK/NFA-89/2 (1989).
10. J. R. Askew and et al., "A general description of the lattice code WIMS," *J. British nucl. Energy Soc.* 5, 564-585 (1966).
11. D. C. Leslie and et al., "Improvements to the theory of resonance escape in heterogeneous fuel I; Regular arrays of fuel rods," *Nucl. Sci. Eng.* 22, 78-86 (1965).
12. M. Segev, "Interpolation of resonance integrals," *Nucl. Sci. Eng.* 17, 113-118 (1981).
13. A. Khairallah and J. Recolin, "Calcul de l' autoprotection resonnante dans les cellules complexes par la methode des sous-groupes," *Proc. Seminar IAEA-SM-154 on Numerical Reactor Calculations*, 305-317, I.A.E.A., Vienna (1972).
14. W. Rothenstein, "Resonance absorption calculations in thermal reactors," *Progr. Nucl. Energy* 5, 95-144 (1980).
15. C. Notari and Z. Garraffo, "Spatial self-shielding for heterogeneous cells," *Ann. Nucl. Energy* 14, 615-618 (1987).
16. R. J. Stamml' er and et al., "HELIOS Methods," Studsvik Scandpower (1998).
17. A. A. Y. Gagarinski and et al., "Water-Moderated Hexagonally Pitched Double Lattices of U(80%)O2 + Cu Fuel Rods and Boron Carbide Rods," HEU-COMP-THERM-008, NEA/NSC/DOC/(95)03/II, Volume II (1995).